Rain Rate and Attenuation Contour Maps for Television Satellite Links in Mauritius

Attenuation losses in satellite communication systems originate from atmospheric losses, which become dominant at frequencies above 5 GHz. By using higher frequencies, communication systems can increase their bandwidth and throughput. However, the drawback is that rain attenuation affects the radio signals at frequencies above 5 GHz. Satellite TV in Mauritius uses the Ku band, and outages are common during rainfall, resulting in significant signal losses and a lower quality of the information. Rainfall causes radio waves to be absorbed and scattered, which lowers the received signal strength. In this work, the ITU-R 837-7 recommendations, Rice Holmberg (RH), and the refined Moupfouma-Martin (RMM) models have been assessed to find the rain rate for one-min integration time from monthly precipitation statistics for the period 1991 to 2020 for the 9 districts of Mauritius. The attenuation of rain has been predicted for the EUTELSAT satellite communication system using Recommendation ITU-R 618-13, the Ramachandran-Kumar (RK) model, and the Yeo-Lee-Ong (YLO) model. Contour maps of precipitation rate and attenuation have been established for the first time for Mauritius, which will be helpful for planning and designing satellite links for the different regions of the country.

Keywords: *Contour map, rain attenuation, ku band, Mauritius*

Introduction

Higher-frequency radio waves are attenuated by the ionosphere because of its electron density [1]. Rain and clouds cause attenuation of high-frequency radio waves. Frequency, geographic location, and elevation angle influence rain attenuation [2, 3, 4]. The ITU R 618-13 (2017) recommends the method used to calculate the attenuation brought on by clouds and precipitation along a slant propagation path needed for the design of earth-satellite communication systems [2]. Link availability for 99.99 percent of the time is frequently desired for the majority of satellite links [2]. A method for forecasting precipitation rate data with a one-minute integration time is suggested in ITU-R P.837-7 [5]. The prediction process proposed can be used for the conversion of monthly available rain data to one-minute integrated rain rate data. Other methods, like the Rice-Holmberg [6] and the refined Moupfouma-Martin models, can also be used for the conversion [7]. Rain rate models are very helpful for determining the point rainfall rate for specific locations, and a number of experimental models are mentioned in the literature [6, 8, 9, 10, 11]. These models include the ITU-R P.837-7 model [5], the Rice and Holmberg (RH) model [6], the Moupfouma model [12], the Moupfouma and Martins model (RMM) [7], and the Crane (1985, 1996, and 2003) models [13, 14, and 15]. The RH model was created using considerable data from many locations worldwide.

This model creates a rain rate distribution from two rain modes. The RH model is found to underestimate rainfall rates below 0.01% [14]. The Moupfouma and Martin model [7] was found to be a better model than the Moupfouma model [12]. Both tropical and temperate climates responded better to this model. Mandeep Singh and al. compared measured rain and attenuation data with the ITU-R model in Malaysia [16]. The RH model performed better than the Kitami, ITU-R, and Moupfouma models [17].

In [18], contour maps for one-minute precipitation rate and rain attenuation were generated for South Africa using the refined Moupfouma model and the ITU-R recommendation model, respectively. In [19], the rainfall rate was determined using the method of RH [6] for satellite links in Nigeria. Mangones et al. [20] applied the ITU-R P.837-7 recommendation, RH [6], and the RMM models to estimate the rain rate for Venezuela. Previous research has demonstrated a number of models for predicting the attenuation of rain for satellite communication systems, like Recommendation ITU-R 618-13 [4], the RK model [21], and the YLO model [22]. Some other studies show a 30% to 40% difference as compared to measured data [23, 24].

When compared to the traditional ITU-R model, experimentally obtained rain attenuation had overestimated results [25]. Tjelta et al. (2017), Kaustav Chakravarty, and Animesh Maitra [26] discovered that the ITU-R model [27] performed well in North America when tested. With the NSS-6 satellite, rain attenuation models were tested in the frequency range of 12 to 40 GHz over the earth–space communication link at urban communities in India. The ITU-R model was found to perform better when the rain rate and frequencies were high [28]. Mangones et al. [20] used the Recommendation ITU-R P.618-13, RK [21], and YLO models [22] for evaluating the rain attenuation in Venezuela with comparable results for rain attenuation. Some recent studies are given in the next paragraph.

Past meteorological data is used in [29] to create a rain prediction model using a rule-based machine learning technique. In [30], the ITU-R P.837 was found to provide good statistical predictions of rainfall rates for Columbia.

The ITU-R is used to calculate the attenuation of radio waves due to rainfall for the estimation of the yearly radio throughput in Budapest, Hungary [31]. Using the ITU-R models for the estimation of rain attenuation in their study [32], a unique architecture of linear precoding was developed for the feeder link of a broadcast satellite system operating with complete frequency reuse in order to greatly increase the possible capacity. In [33], the authors demonstrate an improved adaptive code modulation (ACM) for reducing rainfall fade in Ethiopia using the ITU-R for rain attenuation prediction. In [34], the SC EXCELL model and the Lin model were found to better estimate the attenuation for extremely high-frequency (EHF) terrestrial links than the ITU-R model.

Satellite TV in Mauritius uses the Ku band, and outages are common during rainfall, resulting in significant signal losses and a lower quality of the information. In order to design reliable satellite systems for tropical countries in the southern hemisphere, specifically Mauritius, this paper aims to provide

communication system planners with supplementary information, including contour maps of rain rate and attenuation. In Mauritius, there are 2 main operators that offer satellite television, namely the Parabole group and the Canal Satellite group, which offers Canal Sat. Both use the EUTELSAT satellite in the Ku band. The EUTELSAT satellite operates in the Ku band and has an orbital position of 10° E, a latitude of 20°, and an elevation of 32°. The contour maps established for rain rate and attenuation will help to assess the implementation of satellite coverage in the different regions of Mauritius. The contour maps are generated using the models designed for tropical regions by the ITUR 837-7 recommendation, RH [5], RMM [6], and Chebil-Rahman's [35] model for the $R_{0.01}$ rain rate, and the ITU-R 618-13 [4], the RK [21], and the YLO models [22] for rain attenuation prediction methods. Similar works have been carried out in Nigeria [36], Venezuela [20], Malaysia [35], India [37], South Africa [38], Bangladesh [39], Libya [40], Brazil [41], and Columbia [42].

Proposed System Model

In this section, the prediction models used for the rain rate and attenuation are described. The average monthly temperatures and precipitation from the Climate Change Knowledge Portal [43] for Mauritius from 1991 to 2020 have been used to generate the rain rate and attenuation contour maps from the models described in the following sub-sections. The rain rate and attenuation contour maps are created in ArcGIS 10.5.1 with the use of Spline for data interpolation.

Prediction Methods for Rainfall Rate

The ITU-R P.837-7 [5], the RMM, and the Rice-Holmberg methods have been used to predict the rainfall rate probabilities of exceedance of 0.01%, 0.1% and 0.5% converted to 1-min integration.

The total precipitation and average surface temperature for the period 1991-2020 for Mauritius [43] have been used to calculate the rainfall rate exceeded for a desired average annual probability of exceedance for a given location in Mauritius. The total precipitation is given by equation (1).

$$P(R > R_{ref}) = \frac{\sum_{ii=1}^{12} N_{ii} P_{ii}(R>R_{ref})}{365.25}(\%) \quad (1)$$

where

$$P_{ii}(R > R_{ref}) = P_{0_{ii}} Q\left(\frac{lnln\,(R_{ref}) + 0.7938 - lnln\,(r_{ii})}{1.26}\right)(\%) \quad (2)$$

and

$$Q(x) = \frac{1}{\sqrt{(2\pi)}} \int_x^{\infty} e^{-\frac{t^2}{2}}\, dt$$

$$r_{ii} = 0.5874 e^{0.0883 t_{ii}}\ for\ t_{ii} \geq 0^0 C\ (mm/hr)$$

$$r_{ii} = 0.5874\ for\ t_{ii} < 0^0 C$$

$$P_{0_{ii}} = 100 \frac{MT_{ii}}{24 N_{ii} r_{ii}} (\%)$$

Where *ii* is the month integer, N_{ii} is the monthly days, MT_{ii} is the monthly average total precipitation in mm and t_{ii} is the monthly surface temperature in ^0C.

The rainfall rate, R_{ref}, is modified until 100 $|P(R>Rref)/p - 1| < 0.001$ where *p* is precipitation rate probability of exceedance.

The Rice- Holmberg Model

The complementary cumulative distribution function (CCDF) for which the precipitation rate exceeds R mm/h at a location is given by equation (3).

$$P(r \geq R) = \frac{M}{87.66}[0.03\beta^{-0.003R} + 0.2(1-\beta)(e^{-0.258R} + 1.86e^{-1.63R}] \quad (3)$$

M is the average annual rainfall accumulation (in mm), M1, is the average annual accumulation of thunderstorms or convective rains (in mm). M1 was obtained from the Mauritius Meteorological Services [43]. β=M1/M.

Refined Moupfouma-Martin model

The complementary cumulative distribution function (CCDF) for which the precipitation rate exceeds R mm/h at a location is given by (4) [7, 18, 20].

$$P(r \geq R) = 10^{-2} \left(\frac{R_{0.01}+1}{R+1}\right)^b e^{[u(R_{0.01}-R)]} \quad (4)$$

$$b = \left(\frac{R - R_{0.01}}{R_{0.01}}\right) ln\left(\frac{R_{0.01} + R}{R_{0.01}}\right)$$

$$u = \frac{4ln10}{R_{0.01}} e^{\left[-1.066\left(\frac{R}{R_{0.01}}\right)^{0.214}\right]}$$

where u is calculated for tropical and subtropical climates. R0.01 is the precipitation rate exceeded at 0.01% of time in an average year and is obtained from the Chebil-Rahman model [20]. The equation used to calculate $R_{0.01}$ is given below.

$$R_{0.01} = 12.2903M^{0.2973} \quad (5)$$

where M is the annual cumulative average precipitation (in mm)

Models for Rain Attenuation

Recommendation ITU-R P. 618-13

The ITU-R P. 618-13 [2] recommendation consists mainly of calculating the rain height, slant path length, specific attenuation, effective path length and the predicted attenuation exceeding p% of an average year. The parameters used in this model are the local point precipitation rate, the height above mean sea level of the earth station , h_s, the elevation angle, Θ , wave polarisation, the latitude of the earth station, φ, frequency f and effective radius of the earth are. The steps that follow provide predictions for the attenuation. The earth space factors are given in Figure 1.

Figure 1. *Earth Space Factors [2]*

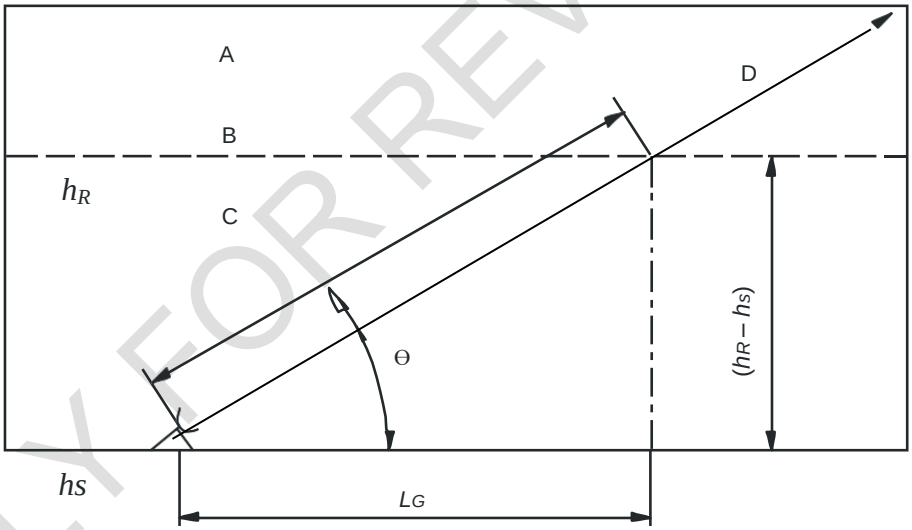

Step 1: The rain height, h_R, is determined as given in [44].
Step 2: If Θ ≥ 5°, L_s, is obtained from:

$$L_s = \frac{(h_R - h_s)}{sin\theta} \text{ km} \quad (6)$$

Else

$$L_s = \frac{2(h_R - h_s)}{\left(sin^2\theta + \frac{2(h_R - h_s)}{R_e}\right)^{\frac{1}{2}} + sin\theta} \text{ km} \quad (7)$$

Step 3: L_G, is calculated from:

$$L_G = L_s \, cos \, cos \, \theta \text{ km} \quad (8)$$

Step 4: Identify the precipitation rate, $R_{0.01}$
Step 5: Using values of alpha and k provided in [45]and $R_{0.01}$, as determined in Step 4, obtain the specific attenuation, R, using:

$$\gamma_R = k(R_{0.01})^{\alpha} \text{ dB/km} \quad (9)$$

Step 6: Find, $r_{0.01}$:

$$r_{0.01} = \frac{1}{1+0.78\sqrt{\left(\frac{L_G\gamma_R}{f}\right)}-0.38\left(1-e^{-2L_G}\right)} \quad (10)$$

Step 7: Find $v_{0.01}$:

$$\varsigma = \tan^{-1}\left(\frac{h_R - h_s}{L_G r_{0.01}}\right)$$

For $\varsigma > \Theta$,

$L_R = \frac{L_G r_{0.01}}{\cos\theta}$ km

Else, $L_R = \frac{h_R - h_s}{\sin\theta}$ km

$$\chi = \{36 - |\varphi|, \quad |\varphi| < 36^0 \; 0, \quad |\varphi| \geq 36^0$$

$$\chi = \begin{cases} 36 - |\varphi|, & |\varphi| < 36^0 \\ 0, & |\varphi| \geq 36^0 \end{cases}$$

$$v_{0.01} = \frac{1}{1+\sqrt{(sin\theta)}\left[31\left(1-e^{-\left(\frac{\theta}{1+\varkappa}\right)}\right)\frac{\sqrt{(L_R\gamma_R}}{f^2}-0.45\right]} \quad (11)$$

Step 8: Find the effective path length:

$$L_E = L_R v_{0.01} \text{ km} \quad (12)$$

Step 9: Find the estimated attenuation for p= 0.01%, using:

$$A_{0.01} = \gamma_R L_E \text{ dB} \quad (13)$$

Step 10: Find the estimated attenuation exceeded for other percentages (p) of an average year:

$$\beta = \begin{cases} 0, & p \geq 1\% \; or \; |\varphi| \geq 36 \\ -0.005(|\varphi| - 36), & p < 1\% \; and \; |\varphi| - 36 \; and \; \theta \geq 25° \\ -0.005(|\varphi| - 36) + 1.8 - 4.25 sin\,\theta, & Otherwise \end{cases}$$

$$A_p = A_{0.01}\left(\frac{p}{0.01}\right)^{-(0.655+0.033ln(p)-0.045lnA_{0.01}-\beta(1-p)sinsin\,\theta)} \text{ dB} \quad (14)$$

Ramachandran-Kumar Model

For use in the tropics, section 2.4.1. model is suggested with modifications to steps 5 to 10 as given below:

$\gamma_{0.01}$, $r_{0.01}$and $v_{0.01}$ switch to γ_B , r_B and v_B respectively.

Step 8: L_E is determined as follows:

$L_E = L_R v_B$ km (15)

Step 9:

For $40° \leq \theta \leq 60°$, $A_B = \gamma_B L_E C_f$ (16)

Else $A_B = \gamma_B L_E$ (dB) (17)

Where $C_f = -0.002\theta^2 + 0.175\theta - 2.3$ (18)

Step 10: Find the estimated attenuation exceeded for p %.

$$A_p = \begin{cases} A_B \left(\frac{p}{0.021}\right)^{-0.5\left(0.655+0.033lnp^2-0.045lnA_B-\beta(0.989-p)sinsin\,\theta\right)}, & p \leq 0.021 \\ A_B \left(\frac{p-0.011}{0.021}\right)^{-0.655-0.033lm(p-0.011)+0.045lnA_B+\beta(0.989-p)sinsin\,\theta}, & 0.021 \leq p < 1 \end{cases} \quad (19)$$

$$\beta = \begin{cases} 0, & p \geq 1\%\ or\ |\varphi| \geq 36 \\ -0.005(|\varphi| - 36), & p < 1\%\ and\ |\varphi| - 36\ and\ \theta \geq 25° \\ -0.005(|\varphi| - 36) + 1.8 - 4.25sin\,\theta, & Otherwise \end{cases}$$

Yeo-Lee-Ong Model

Yeo. Lee and Ong [22] also proposed modifications to steps 6 to 10 of the section 2.4.1 model for tropical regions as given below.

Step 6:

$$r = \frac{1}{\frac{0.3979}{sinsin\,\theta}+0.0021R_{0.01}(H-h_s)-0.0185f+0.2337} \quad (20)$$

Where H is the rain height in km.

Step 7:

$$A_{0.01} = \gamma_{0.01} L_S r \text{ dB} \quad (21)$$

Step 8: The estimated attenuation exceeded for p % is calculated from:

$$A_p = A_{0.01}\left(\frac{p}{0.01}\right)^{(-1.0063-0.0591lnp-0.1317lnA_{0.01}-\beta(1-p)sinsin\,\theta)} \text{ dB} \quad (22)$$

$$\beta = \begin{cases} 0, & p < 1\%\ and\ |\varphi| - 36° \\ -0.005(|\varphi| - 36°), & p < 1\%\ and\ |\varphi| - 36°\ and\ \theta \geq 25° \\ -0.005(|\varphi| - 36) + 1.7 + 7.85sin\,\theta, & Otherwise \end{cases} \quad (23)$$

Results and Discussions

Precipitation Contour Maps for Mauritius

There are 9 districts in Mauritius: Flacq, Grand Port, Moka, Pamplemousses, Plaines Wilhems, Port Louis, Rivière du Rempart, Black River, and Savanne, as shown in Figure 2. Table 1 shows the annual average temperature and precipitation data for Mauritius for the period 1991–2020. Mauritius has a tropical,

warm climate that is moderated by southeast trade winds. The direction of the trade winds has a large influence on the amount of rain that falls on the island; the eastern part of the island is relatively rainier than the western part.

Figure 2. *Districts of Mauritius*

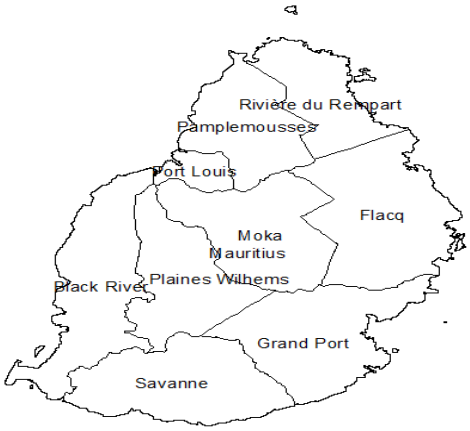

Table 1. *Temperature and Precipitation Data for Mauritius for the Period 1991-2020*

Station	Latitude (^{0}E)	Longitude (^{0}S)	Altitude (m)	Annual Average temperature (^{0}C)	Annual Average precipitation (mm)
Flacq	57.7144	20.1897	131.7	23.79	1781.8
Black River	57.38417	20.4158	77.16	23.1	1704.73
Savanne	57.5	20.4667	224.38	23.3	1772.67
Riviere Du Rempart	57.68472	20.1031	44.66	23.79	1781.8
Port Louis	57.49638	20.1653	6.72	23.53	1752.38
Plaines Wilhems	57.48536	20.3055	419.25	23.35	1732.18
Pamplemousses	57.58159	20.1095	78.57	23.79	1781.66
Moka	57.5	20.2167	343.21	23.74	1775.71
Grand Port	57.66657	20.3852	160.56	23.79	1781.8

Table 2 shows the rainfall rates for probability of exceedance at 0.01%, 0.1%, and 0.5% time of exceedance using the ITU-R 837-7 Annex 1 recommendation, Rice-Holmberg, and refined Moupfouma-Martin models. The rain rates are converted to 1-min integration. We can observe from the results obtained that the rainfall rate increases for a higher percentage of time

than expected. Also, the rainfall rates are higher for the refined Moupfouma-Martin model as compared to the Rice-Holmberg and ITU-R 837-7 models.

Table 2. *Rainfall Rate for 0.01%, 0.1% and 0.5% Probability of Exceedance*

	ITU-R P.837-7			**Refined Moupfouma-Martin**			**Rice-Holmberg**		
	0.01%	**0.1%**	**0.5%**	**0.01%**	**0.1%**	**0.5%**	**0.01%**	**0.1%**	**0.5%**
Flacq	**77.6**	16.59	7.3	113.78	41.01	13.66	91.12	20.28	8.07
Black River	73.9	15.85	7.3	112.29	40.48	13.49	75.04	16.81	7.9
Savanne	75.7	16.22	7.17	113.61	40.95	13.64	88.45	19.42	8.05
Riviere Du Rempart	77.7	16.62	7.27	113.78	41.01	13.66	90.97	20.28	7.99
Port Louis	76.4	16.32	6.97	113.22	40.81	13.6	75	16.92	8.02
Plaines Wilhems	75.1	16.12	7.05	112.83	40.67	13.55	91.2	20.22	7.93
Pamplemousses	**77.6**	16.59	7.15	113.78	41.01	13.66	82.22	18.02	8.09
Moka	77.3	16.55	7.34	113.66	40.97	13.65	91.39	20.37	8.05
Grand Port	**77.8**	16.62	7.31	113.78	41.01	13.66	91.13	20.28	8.07

Figures 3 to 11 show the contour maps for the rainfall rates for the ITU-R 837-7, Rice-Holmberg, and refined Moupfouma-Martin models for 0.01%, 0.1%, and 0.5% probability of exceedance. It can be seen that the eastern part of the country (Moka-Flacq, Grand Port) has a higher rainfall rate and the western part (Port Louis, Black River) has a lower rainfall rate. This is true for all the probabilities of exceedance considered. We can also note that the rainfall rate is lower in the north and west coastal regions of Mauritius, where the elevation above sea level is low. The rainfall rate increases for regions that are at a higher elevation above sea level, as expected.

Figure 3. *Precipitation rate (mm/hr) contour map for ITU-R P. 837-7 recommendation (p=0.01%)*

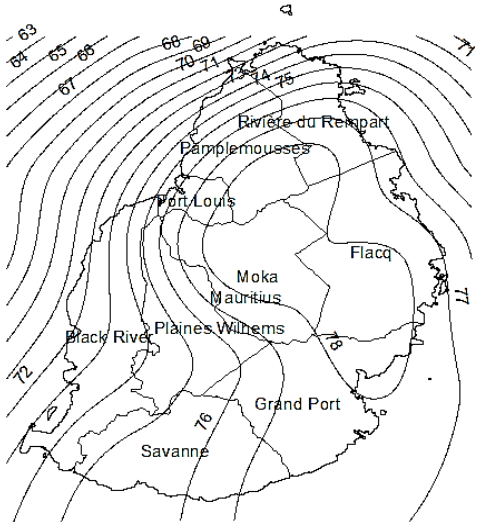

Figure 4. *Precipitation rate (mm/hr) contour map for Rice-Holmberg model (p=0.01%)*

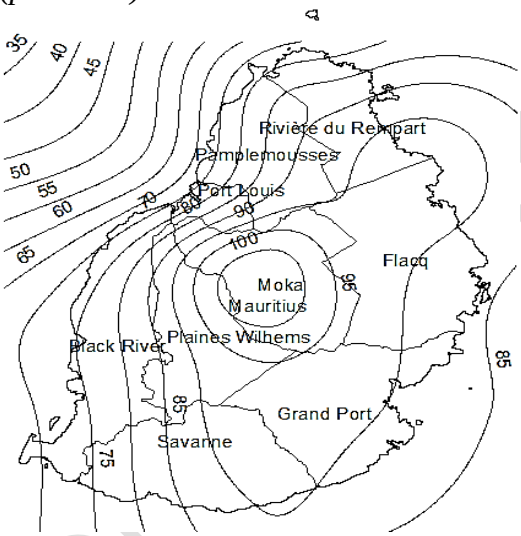

Figure 5. *Precipitation rate (mm/hr) contour map for Refined Moupfouma-Martin model (p=0.01%)*

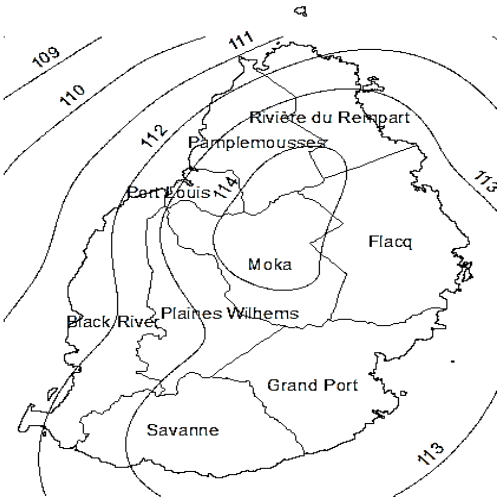

Figure 6. *Precipitation rate (mm/hr) contour map for ITU-R P. 837-7 recommendation (p=0.1%)*

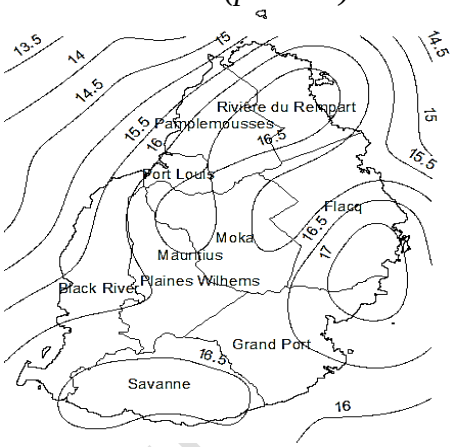

Figure 7. Precipitation rate (mm/hr) contour map for Rice-Holmberg model (p=0.1%)

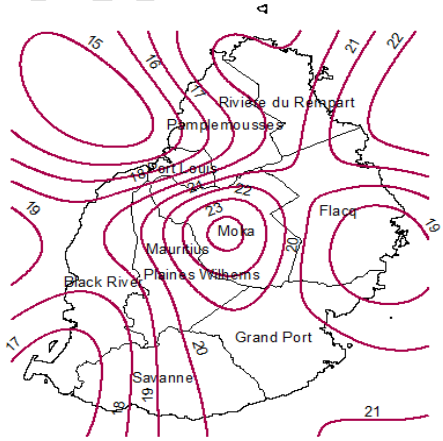

Figure 8. *Precipitation rate (mm/hr) contour map for ITU-R P.837-7 recommendation (p=0.5%)*

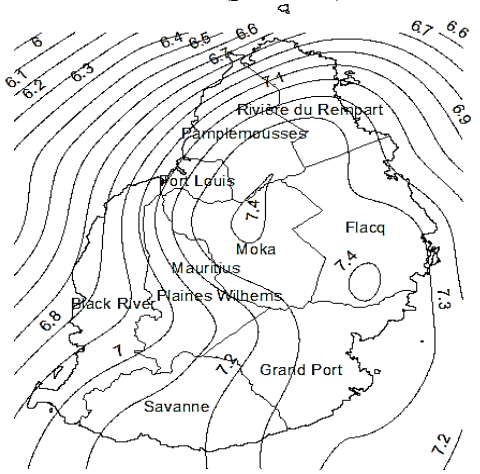

Figure 9. *Precipitation rate (mm/hr) contour map Refined Moupfouma-Martin model (p=0.1%)*

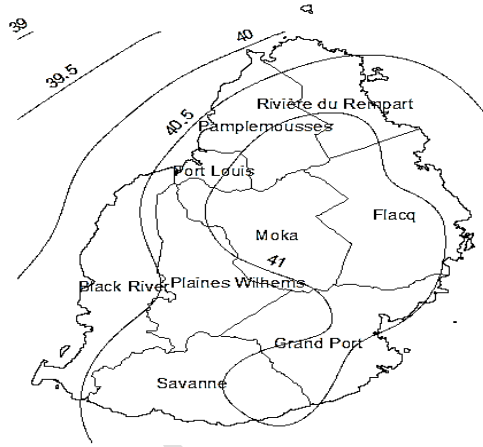

Figure 10. *Precipitation rate (mm/hr) contour map for Rice-Holmberg model (p=0.5%)*

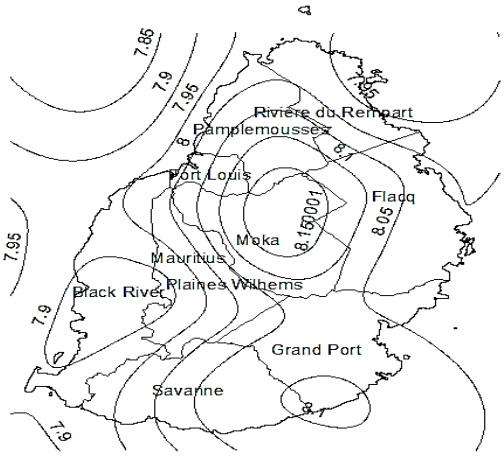

Figure 11. *Precipitation rate (mm/hr) contour map for Refined Moupfouma-Martin model (p=0.5%)*

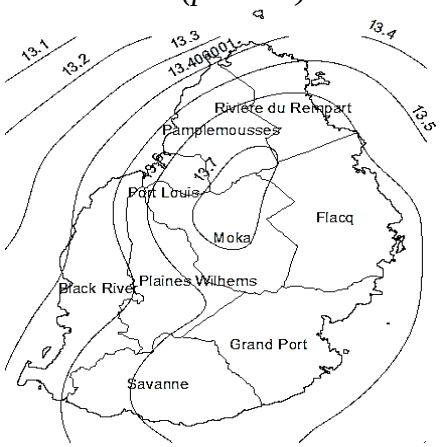

Rain Attenuation Contour Maps for Mauritius

The Ramachandran-Kumar and the Yeo models have similar steps as compared to the ITU-R P. 618-13, except that the equations used for calculating the attenuation are different. The attenuation levels have been calculated for the EUTELSAT satellite with a 10° E orbital position, latitude of 20°, and elevation of 32°, operating in the Ku band at a frequency of 12 GHz. Figures 12 to 20 show the attenuation contour maps from the ITU-R, Ramachandran-Kumar, and Yeo methods. All indicate that attenuation is slightly higher in the country's east and south. The districts concerned are those of Flacq, Savanne, and Grand Port. Because of the higher level of precipitation, the east parts of the Moka and Plaines Wilhems districts are also affected. The attenuation is relatively lower in the north and west. The regions concerned are those of Grand Baie, Cap Malheureux, Bambous, Flic en Flac, Black River, and Tamarin. Precipitation has less attenuated some west parts of the Plaines-Wilhems district, such as Quatre Bornes.

It can also be observed from these figures that the ITU-R model gives the lowest values of attenuation as compared to the Ramachandran-Kumar and the Yeo models. We can also note that the Ramachandran-Kumar model gives the highest attenuation values as compared to the ITU-R recommendation and the Yeo-Lee-Ong models. It is difficult to know which model gives the most accurate results of attenuation when no actual measurements have been done for this satellite link. However, it is important to know about these attenuations in different regions of the country to predict service availability and interruptions in this satellite link since competitors are providing no interruptions in the TV service through fiber optic cables. RF changes could be considered to reduce attenuation levels and improve link availability at all times.

Figure 12. *Attenuation (dB) for ITU-R P.618-13 recommendation (p=0.01%)*

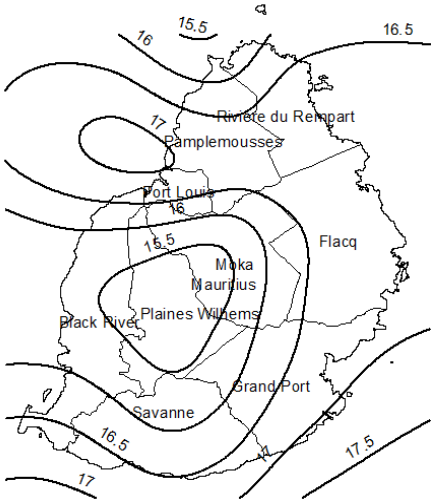

Figure 13. *Attenuation (dB) contour map for RK model (p=0.01%)*

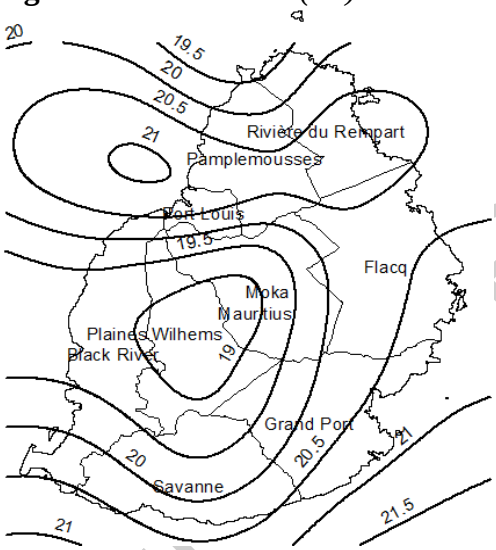

Figure 14. *Attenuation (dB) contour map for YLO model (p=0.01%)*

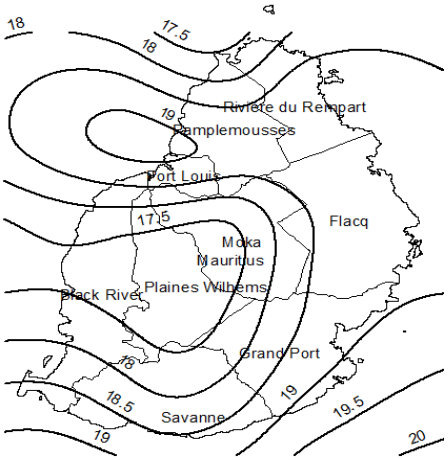

Figure 15. *Attenuation (dB) contour map for ITU-R P.618-13 recommendation (P=0.1%)*

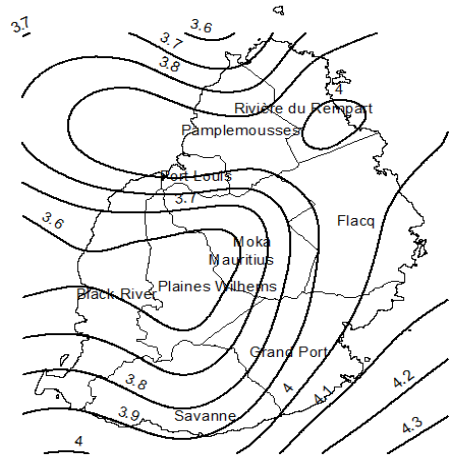

Figure 16. *Attenuation (dB) contour map for YLO model (p=0.1%)*

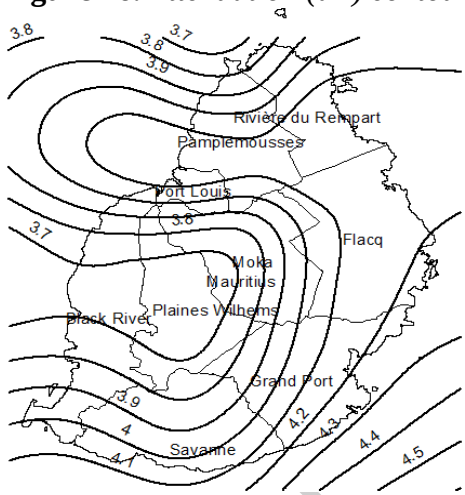

Figure 17. *Attenuation (dB) contour map for ITU-R P.618-13 recommendation (p=0.5%)*

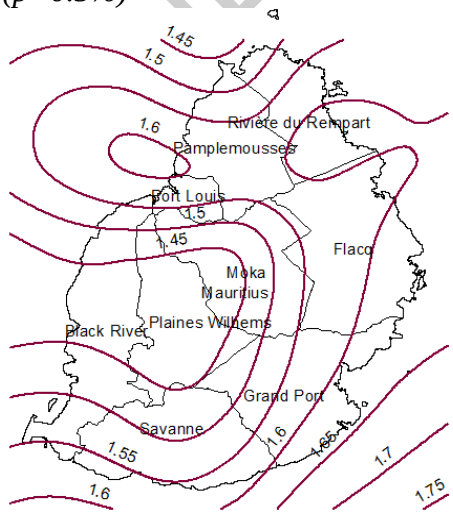

Figure 18. *Attenuation (dB) contour map for RK model (p=0.1%)*

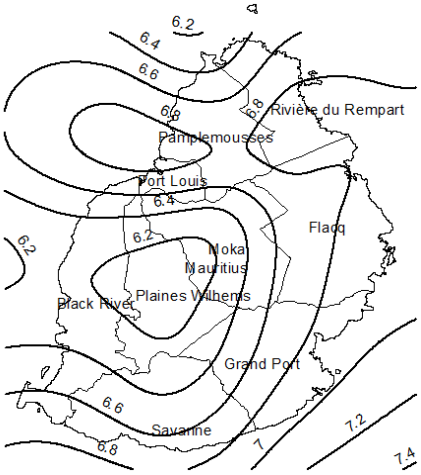

Figure 19. *Attenuation (dB) contour map for YLO model (p=0.5%)*

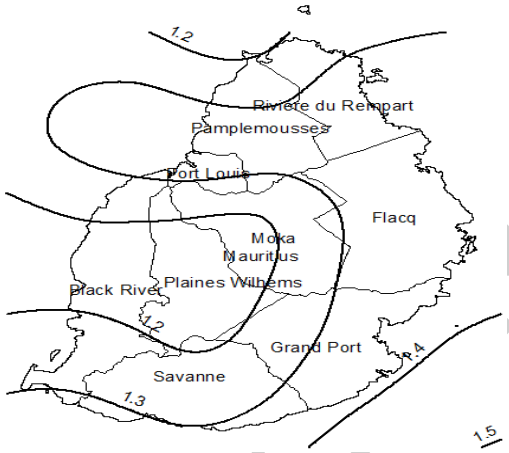

Figure 20. *Attenuation (dB) contour map for RK model (p=0.5%)*

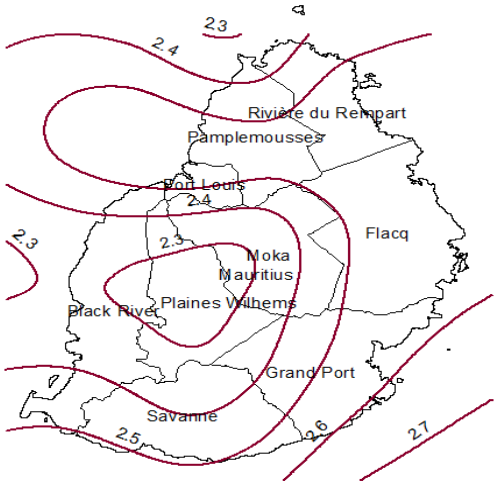

We can also observe from Figures 12 to 20 that the maximum average difference in attenuation of 3.7 dB for a 0.01% exceedance probability is between

the Ramachandran-Kumar model and the ITUR-618-13 recommendation. This average difference decreases to 2.8 dB and then to 1 dB for 0.1% and 0.5% of the exceedance probability, respectively. It is also to be noted from these figures that the maximum average difference in attenuation of 2 dB for a 0.01% exceedance probability is between the Yeo-Lee-Ong model and the ITUR-618-13 recommendation. This average difference decreases to 0.14 dB and then to -0.25 dB for 0.1% and 0.5% of exceedance probability, respectively. The difference in attenuation between the Yeo-Lee-Ong model and the ITUR-618-13 recommendation is negligible for 0.1% and 0.5% of exceedance probability.

Conclusions

For the first time, the contour maps for the rainfall rates from the ITU-R 837-7, Rice-Holmberg, and refined Moupfouma-Martin models for 0.01%, 0.1%, and 0.5% probability of exceedance have been shown for Mauritius. It can be seen that the eastern part of the country (Moka-Flacq, Grand Port) has a higher rainfall rate and the western part (Port Louis, Black River) has a lower rainfall rate. Attenuation contour maps from the ITU, ARKM, and Yeo methods all show that attenuation is slightly higher in the country's east and south. The districts concerned are those of Flacq, Savanne, and Grand Port. Because of the higher level of precipitation, the east parts of the Moka and Plaines Wilhems districts are also affected. It is also observed that there is a slight variation in the attenuation across the country due to its size, topology, and distance from the satellite. The rain rate and attenuation derived from these methods provide preliminary data for planning and designing future satellite links for the country and also for developing countermeasures to rain attenuation so as to provide high-quality service to subscribers. As technology advances, real-time attenuation values for measured rainfall rates could be measured to find the most accurate prediction method.

References

[1] Dabas, R..: Ionosphere and its influence on radio communications. Resonance. 5. 28-43(2012). https://doi.org/10.1007/BF02867245

[2] International Telecommunication Union – Radiocommunication, Recommendation P.618-13: propagation data and prediction methods required for the design of earth-space telecommunication systems, Geneva, Switzerland, (2017)

[3] Zubair, M., Janjua, Z., Khan, S., Nasir, J.: Atmospheric influences on satellite communications. Przeglad Elektrotechniczny. 87 (3), (2011)

[4] Ippolito, L.J.: Radio propagation for space communications systems, in Proceedings of the IEEE, 69, 6, 697-727, (1981). https://doi.org/10.1007/BF0286724510.1109/PROC.1981.12049

[5] International Telecommunication Union – Radiocommunication, Recommendation P.837-7: Characteristics of precipitation for propagation modelling, Geneva, Switzerland, (2017)

[6] Rice, P.L., Holmberg N.R.: Cumulative Time Statistics of Surface-Point Rainfall Rates. IEEE Transactions on Communications. COM-21, 10, 1131-1136 (1973)
[7] Moupfouma, F., Martins, S.: Modeling of the rainfall rate cumulative distribution for design of satellite and terrestrial communication systems. International Journal of Satellite Communication. 13(2) 105-115 (1995)
[8] Olsen, R.L.: Radio climatological Modelling of Propagation Effects in Clear-Air and Precipitation Conditions. Recent Advances and Future Directions, Radio Africa (1999)
[9] Dissanayake, A, Allnutt, J., Haidara, F.: A prediction model that combines rain attenuation and other propagation impairments along earth-satellite paths. Online Journal of Space Communication. Issue No. 2, 1-29 (2002)
[10] Ojo, J.S., M.O. Ajewole, and S.K. Sarkar: Rain rate and rain attenuation Prediction for Satellite Communication in Ku and Ka Bands Over Nigeria. Progress In Electromagnetics Research B. 5, 207-223 (2008).
[11] Chun, Ooi, Mandeep, Jit: Empirical methods for converting rainfall rate distribution from several higher integration times into a 1-minute integration time in Malaysia. Geofizika. 30. 143-154 (2013)..
[12] Moupfouma, F.: More about rainfall rates and their prediction for radio systems. IEEE Proceedings. 134 (6), Pt. H, 527-537(1987)
[13] Crane, R.K.: Evaluation of Global and CCIR models for estimation of rain rate statistics. Radio Science. 20, 4, 865-879 (1985)
[14] Crane, R. K. Electromagnetic Wave Propagation through Rain. Wiley Interscience, New York (1996)
[15] Crane, R. K.: Propagation Handbook for Wireless Communication System Design. CRC Press, New York (2003).
[16] Singh, M., Hassan, S.I., Ain, M.F.: Rainfall Attenuation and Rainfall Rate Measurements in Malaysia Comparison with Prediction Models. American Journal of Applied Sciences. 4, (2007). https://doi.org/10.3844/ajassp.2007.5.7.
[17] Obiyemi, O.O., Ojo, J., Ibiyemi, T.S.: Performance Analysis of Rain Rate Models for Microwave Propagation Designs over Tropical Climate. Progress in Electromagnetics Research. 39, 115-122 (2014). https://doi.org/10.2528/PIERM14083003
[18] Ojo, J.S., Owolawi, P.A.: Development of one-minute rain-rate and rain-attenuation contour maps for satellite propagation system planning in a subtropical country: South Africa. Advances in Space Research. 54, 8, 1487-1501(2014). https://doi.org/10.1016/j.asr.2014.06.028
[19] Omotosho, Temidayo, Oluwafemi, C.: One-minute rain rate distribution in Nigeria derived from TRMM satellite data. Journal of Atmospheric and Solar-Terrestrial Physics. 71. 625-633 (2009). https://doi.org/10.1016/j.jastp.2009.02.003.
[20] Mangones, A., García P., Tovio, J.M.T., Ramírez, E.J., Rivera, S.O.C., Zapata J.V., Rodriguez J.D.F., Molina, L.M.R.: Rainfall rate and rain attenuation contour maps for preliminary "Simon Bolivar" satellite links planning in Venezuela. DYNA. 86. 30-39 (2019). https://doi.org/10.15446/dyna.v86n209.73774
[21] Ramachandran, V., Kumar, V.: Modified rain attenuation model for tropical regions for Ku-band signals. Int. J. Satell. Commun. Netw. 25(1), 53-67 (2007). https://doi.org/10.1007/BF0286724510.1002/sat.846
[22] Yeo, J.X., Lee, Y.H., Ong, J.T.: Rain attenuation prediction model for satellite communications in tropical regions. IEEE Trans. Antennas Propag. 62(11), 5775-5781 (2014). https://doi.org/10.1007/BF0286724510.1109/TAP.2014.2356208
[23] Dissanayake A., Allnutt, J.F.: Haidara A prediction model that combines rain attenuation and other propagation impairment along earth-satellite paths. IEEE Trans. Antennas Propagat. 45, 1558-1564 (1997)

[24] Luini, L., Capsoni, C.: MultiEXCELL: a new rain field model for propagation applications
IEEE Trans. Antennas Propagat. 59 (11), 4286-4300 (2011)
[25] Chakraborty, S., Verma, P., Paudel, B., Das, S.: Modeling of Ka-band slant path rain attenuation for hilly tropical region, Advances in Space Research. 70, 3, 601-609 (2022). https://doi.org/10.1016/j.asr.2022.05.002
[26] Chakravarty, K., Maitra, A.:Rain attenuation studies over an earth–space path at a tropical location. J. Atmos. Sol.-Terr. Phys. 72 (1), 135-138 (2010)
[27] International Telecommunication Union – Radiocommunication, Recommendation P.618-12: propagation data and prediction methods required for the design of earth-space telecommunication systems, (2015)
[28] Panchal, P., Joshi, R.:Performance Analysis and Simulation of Rain Attenuation Models at 12–40 GHz Band for an Earth Space Path over Indian Cities. Procedia Computer Science. 79, 801-808 (2016). https://doi.org/10.1016/j.procs.2016.03.110
[29] Anwar, M., Nugrohadi, S., Tantriyati, V., Windarni, V.:Rain Prediction Using Rule-Based Machine Learning Approach. Advance Sustainable Science, Engineering and Technology. 2, (2020). https://doi.org/10.1007/BF0286724510.26877/asset.v2i1.6019
[30] Emiliani, L., Luini, L., Rolon, A.: One-minute integrated rainfall rate statistics from a rain gauge network in Colombia: Accuracy of prediction methods. Electron. Lett. 56, 17, 859-861(2020)
[31] Hilt, A.:Throughput Estimation of K-zone Gbps Radio Links Operating in the E-band. Journal of Microelectronics, Electronic Components and Materials. 52, 129 – 39 (2022)
[32] Guidotti, A., Sacchi, C., Vanelli-Coralli, A.:Feeder Link Precoding for Future Broadcasting Services. IEEE Transactions on Aerospace and Electronic Systems. 58, 4, 3126-3146 (2022). https://doi.org/10.1007/BF0286724510.1109/TAES.2022.3144243
[33] Woldamanuel, E.M., Diba, F.D.: Enhanced adaptive code modulation for rainfall fade mitigation in Ethiopia. J Wireless Com Network 2022, 8 (2022). https://doi.org/10.1186/s13638-021-02085-0
[34] Luini, L., Roveda, G., Zaffaroni, M., Costa, M., Riva, C. G.: The Impact of Rain on Short E -Band Radio Links for 5G Mobile Systems: Experimental Results and Prediction Models. IEEE Transactions on Antennas and Propagation, 68, 4, 3124-3134 (2020). https://doi.org/10.1007/BF0286724510.1109/TAP.2019.2957116
[35] Chebil, J., Rahman, T.A.: Development of 1 min rain rate contour maps for microwave applications in Malaysia peninsula. Electron. Lett. 35(20), 1172-1174 (1999). https://doi.org/10.1007/BF02867245 10.1049/el:19991188
[36] Ojo, J., Ajewole, O., Sarkar, S.: Rain rate and rain attenuation prediction for satellite communication in Ku and Ka bands over Nigeria. Progress in Electromagnetics Research. 5, 207-223 (2008). https://doi.org/10.1007/BF028672450.2528/PIERB08021201
[37] Kestwal, M.C., Joshi, S., Garia L.S.: Prediction of rain attenuation and impact of rain in wave propagation at microwave frequency for tropical region (Uttarakhand, India). Int. J. Microw. Sci. Technol. 1-6. (2014). https://doi.org/10.1155/2014/958498
[38] Ojo, J. S., Ajewole, M. O., Emiliani, L.D.: One-Minute Rain-Rate Contour Maps for Microwave-Communication-System Planning in a Tropical Country: Nigeria. IEEE Antennas and Propagation Magazine. 51, 5, pp. 82-89 (2009)
[39] Imran, A.Z.M., Islam, M.T., Gafur, A., Rabby, Y.W.: Rain attenuation prediction analysis and contour map design over Bangladesh. Proceedings of the 18th International Conference on Computer and Information Technology (ICCIT 2015).

Dhaka, Bangladesh, 208-212 (2015). https://doi.org/10.1109/ICCITechn.2015.7488069

[40] Islam, M.R., Budalal, A.A.H., Habaebi, M.H., Badron, K., Ismail, A.F.: Performance analysis of rain attenuation on earth-to-satellite microwave links design in Libya. Proceedings of the 6th International Conference on Mechatronics (ICOM 2017). Kuala Lumpur, Malaysia,1-6 (2017)

[41] Fialho, M.R.B., Silva, R.M.L., Pontes, M.S., Oliveira, C.H.R. and Gonsioroski, L.H., Mapas de contorno da taxa de chuva utilizando os históricos de dados acumulados de precipitação no Estado do Maranhão para modelagem de fenômenos radiometeorológicos, Anais do XXXIV Simpósio Brasileiro de Telecomunicações eProcessamento. 148-151 (2016)

[42] Emiliani, L.D., Agudelo, J., Gutierrez, E., Fradique-Mendez C.: Development of rain-attenuation and rain-rate maps for satellite system design in the Ku and Ka bands in Colombia. IEEE Antennas Propag. Mag. 46(6), 54-68 (2004). https://doi.org/10.1109/MAP.2004.1396736

[43] Climate Change Knowledge Portal. https://climateknowledgeportal.worldbank.org/country/mauritius/climate-data-historical. Accessed 06 July 2022.

[44] International Telecommunication Union – Radiocommunication, Recommendation P.839-3: Rain height model for prediction methods.

[45] RECOMMENDATION ITU-R P.838-3: Specific attenuation model for rain for use in prediction methods.